

Application of Differential Evolution Algorithm on Self-Potential Data

Xiangtao Li^{1,2}, Minghao Yin^{1,2}*

1 Faculty of Chemistry, Northeast Normal University, Changchun, People's Republic of China, 2 College of Computer Science, Northeast Normal University, Changchun, People's Republic of China

Abstract

Differential evolution (DE) is a population based evolutionary algorithm widely used for solving multidimensional global optimization problems over continuous spaces, and has been successfully used to solve several kinds of problems. In this paper, differential evolution is used for quantitative interpretation of self-potential data in geophysics. Six parameters are estimated including the electrical dipole moment, the depth of the source, the distance from the origin, the polarization angle and the regional coefficients. This study considers three kinds of data from Turkey: noise-free data, contaminated synthetic data, and Field example. The differential evolution and the corresponding model parameters are constructed as regards the number of the generations. Then, we show the vibration of the parameters at the vicinity of the low misfit area. Moreover, we show how the frequency distribution of each parameter is related to the number of the DE iteration. Experimental results show the DE can be used for solving the quantitative interpretation of self-potential data efficiently compared with previous methods.

Citation: Li X, Yin M (2012) Application of Differential Evolution Algorithm on Self-Potential Data. PLoS ONE 7(12): e51199. doi:10.1371/journal.pone.0051199

Editor: Jérémie Bourdon. Université de Nantes. France

Received August 25, 2012: Accepted October 30, 2012: Published December 11, 2012

Copyright: © 2012 Li, Yin. This is an open-access article distributed under the terms of the Creative Commons Attribution License, which permits unrestricted use, distribution, and reproduction in any medium, provided the original author and source are credited.

Funding: This research is fully supported by Opening Fund of Top Key Discipline of Computer Software and Theory in Zhejiang Provincial Colleges at Zhejiang Normal University under Grant No. ZSDZZZZXK37 and the Fundamental Research Funds for the Central Universities Nos. 11CXPY010. The funders had no role in study design, data collection and analysis, decision to publish, or preparation of the manuscript.

Competing Interests: The authors have declared that no competing interests exist

* E-mail: Minghao.yin1@gmail.com

Introduction

The self-potential (SP) method is one of the most important optimization problems in geophysics, which is on the basis of the measurement of natural occurring potential difference generated chief from electrochemical, electro kinetic and thermoelectric sources. The SP method has been used in a wide range of applications in geophysics, including prospecting purposes [1,2], archaeology [3], engineering problem [4], cave detection [5,6] and geothermal exploration [7,8]. In some conditions, the SP anomaly can be defined by a single polarize body assuming a model of simple geometry like a sphere, a horizontal or vertical cylinder or an inclined sheet. During the past decade, we have viewed different kinds of methods advanced to handle the SP problem: the method of characteristic points [9]; the curve matching method [10,11]; the method of least square approaches [12,13]; the method of derivative analysis and gradients [14]. On the other hand, other techniques have also been used on such as a numerical gradient method, direct interpretation. These techniques can be categorized into two parts: derivative-based method and global search method.

Recently, the differential evolution algorithm [15] has been proposed as a simple and powerful population-based stochastic optimization, which is originally motivated by the mechanism of natural selection. This algorithm searches solutions using three basic operators: mutation, crossover and greedy selection. Mutation is used to generate a mutant vector by adding differential vectors obtained from the difference of several randomly chosen parameter vectors to the parent vector. After that, crossover operator generates the trial vector by combining the parameters of

the mutated vector with the parameters of a parent vector selected from the population. Finally, according to the fitness value, selection determines which of the vectors should be chosen for the next generation by implementing one-to-one completion between the generated trail vectors and the corresponding parent vectors. In order to accelerate the convergence speed and avoid the local optima, several variations of DE have been proposed to enhance the performance of the standard DE recently. Moreover, DE has been proved to be really efficient when solving real world problems [16–23].

In this paper, we will use the differential evolution to perform the SP method for mineral exploration to find some model parameters. In this study, SP data can be interpreted as a simple geometrical body approximation including a sphere, cylinder, dyke and so on. Then we use our algorithm to estimate the SP data such as Süleymanköy anomaly, Weiss anomaly and Nalbant cesmesi anomaly. In order to demonstrate the advantages of the proposed design, the results obtained are compared with other state-of-the-art approaches. The experimental results show that the DE algorithm is very competitive.

Materials and Methods

0.1 Formulation of the Problem

Generally speaking, the inverse problem can be described as follows:

$$d = G(m) \tag{1}$$

where d represents a set of observations and m denotes a set of model parameters, and G is a non-linear forward operator. The main purpose of the process is estimated between observed data and correct parameters of a chosen model. Eq.(1) is ill posed, because of the forward operator is non-linear one. Eq. (1) can also be defined as follows:

$$||d - G(m)|| < \text{tol} \tag{2}$$

where tol is a predetermined threshold value such as 0.001. Eq (2) is effective for any sampling problem.

The SP anomaly at any point P(x) over a sphere or a cylinder-like body can be described in Figure 1. Figure 1 shows the geometry of a sphere and horizontal cylinder in a medium. The following denotation can be used [24].

$$v(x_i,z) = p \frac{(x_i - D)\cos(\theta) - h\sin(\theta)}{((x_i - D)^2 + h^2)^q} + kx_i + c$$
 (3)

where P is electrical dipole moment, x_i is the coordinate of an estimation point at the outside along the profile. θ is the polarization angle and h is the deepness from the beginning. k is the electric current dipole moment, which denotes the base slope and C represents the base level. The shape factors q is 1.5 and 1.0 for a sphere and cylinder, respectively. In section 4, we will investigate to find model parameters of synthetic data and noise added data by using the differential evolution algorithm.

0.2 Differential Evolution Algorithm

Differential Evolution (DE) [15] is a population based stochastic search algorithm for solving optimization problems in continuous space. Different from other algorithms, DE uses the distance and direction information from current population to guide its further search. The fundamental crucial idea behind DE is a scheme for producing trial vectors according to the manipulation of target vector and difference vector. If the trail vector yields a lower objective function than a predetermined population member, the newly generated trail vector will replace the vector and be compared in the following generation.

The algorithm begins with a randomly initiated population which utilize NP D-dimension parameter vector within constrained by the prescribed minimum and maximum bounds.

$$\overrightarrow{X}_{\min} = \{x_{1,\min}, x_{2,\min}, \cdots, x_{D,\min}\}$$

$$\overrightarrow{X}_{\text{max}} = \{x_{1, \text{max}}, x_{2, \text{max}}, \cdots, x_{D, \text{max}}\}$$

Therefore, we may generate the jth component of the ith vector as.

$$x_{j,i,0} = x_{j,\min} + rand_{i,j}[0,1] \cdot (x_{j,\max} - x_{j,\min})$$

Where $rand_{i,j}[0,1]$ is a uniformly distribution random number between 0 and 1. i = 1, ..., NP and j = 1,...,D.

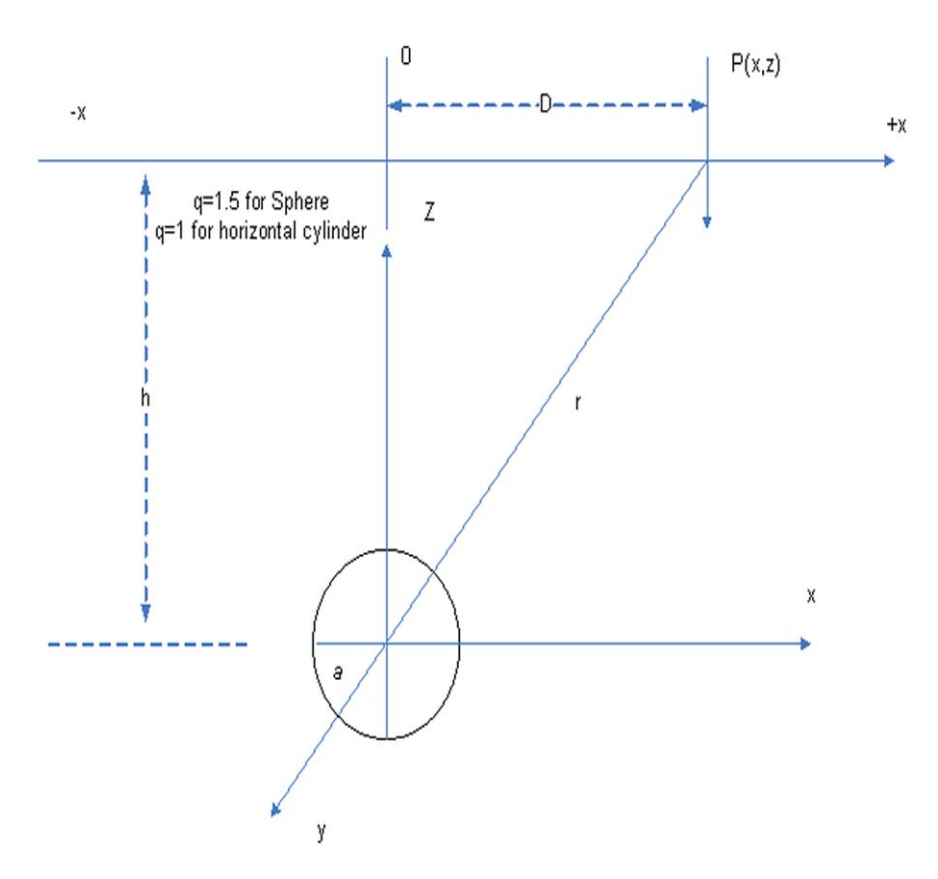


Figure 1. Two simple geometrical bodies under the surface. doi:10.1371/journal.pone.0051199.q001

Table 1. Comparison of true and estimated parameters of SP anomaly.

Parameter Elect.dip.mom.		PSO				DE				
	True	Estimated	Statistics of PSO		Estimated	Statistics of DE				
	100,000	99,9994.0000	Successes	26/30	100,000	Successes	30/30			
Distance	40	40.0001	Mean iter.	59.69	40	Mean iter.	51.70			
Depth	10	9.9950	Std. iterations	27.22	10	Std. iterations	14.23			
Pol. angle(degree)	60	60.0050	Mean func. eval.	18207.69	60	Mean func. eval.	15810.00			
Base slope	0	0.0011	Std func. eval.	8166.95	5.2255e-005	Std func. eval.	4270.46			
Base level	0	-0.1102	Std RMS	3.20	-0.0017318	Std RMS	1.10			
			Mean RMS	1.73		Mean RMS	0.42			
			Min RMS	0.02697		Min RMS	0.0015785831			

doi:10.1371/journal.pone.0051199.t001

After initialization, mutation vectors $V_{i,G}$ are generated according to each population member or target vector $X_{i,G}$ in current population. In the standard DE algorithm, five differential mutation strategies can be used with one of two different crossover methods. There are listed in the following:

"DE/rand/1".

$$V_{i,G} = X_{r_1,G} + F \cdot (X_{r_2,G} - X_{r_3,G})$$

"DE/best/1".

$$V_{i,G} = X_{best,G} + F \cdot (X_{r_1,G} - X_{r_2,G})$$

"DE/current-to-best/1".

$$V_{i,G} = X_{i,G} + F \cdot (X_{best,G} - X_{i,G}) + F \cdot (X_{r_1,G} - X_{r_2,G})$$

"DE/best/2".

$$V_{i,G} = X_{best,G} + F \cdot (X_{r_1,G} - X_{r_2,G}) + F \cdot (X_{r_3,G} - X_{r_4,G})$$

"DE/rand/2".

$$V_{i,G} = X_{r_1,G} + F \cdot (X_{r_2,G} - X_{r_3,G}) + F \cdot (X_{r_4,G} - X_{r_5,G})$$

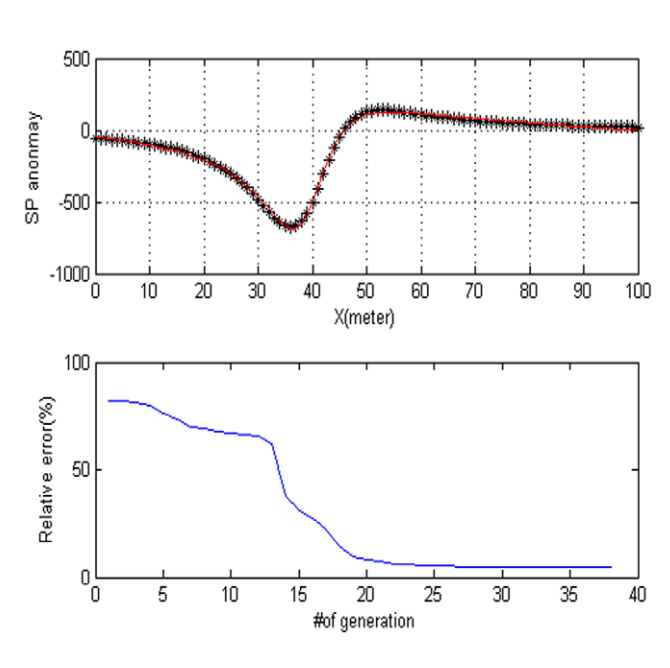


Figure 2. Noise-free data for a cylinder. (a) Dotted lines synthetic data for a cylinder. Estimated SP anomaly is illustrated by solid line. (b) The convergence rate of the DE algorithm. doi:10.1371/journal.pone.0051199.q002

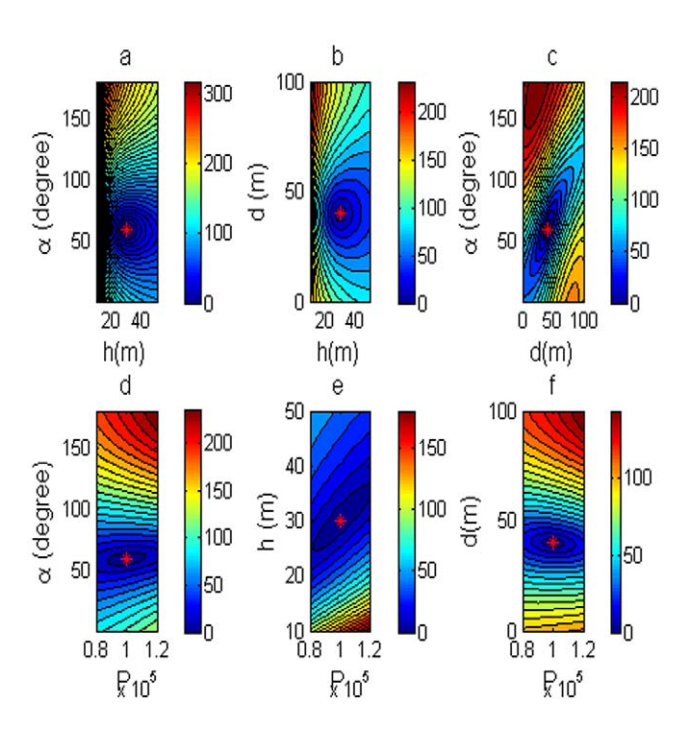


Figure 3. Contour maps of low misfit areas with noise free data. Two of six parameters are variable, rest of them are fixed. doi:10.1371/journal.pone.0051199.g003

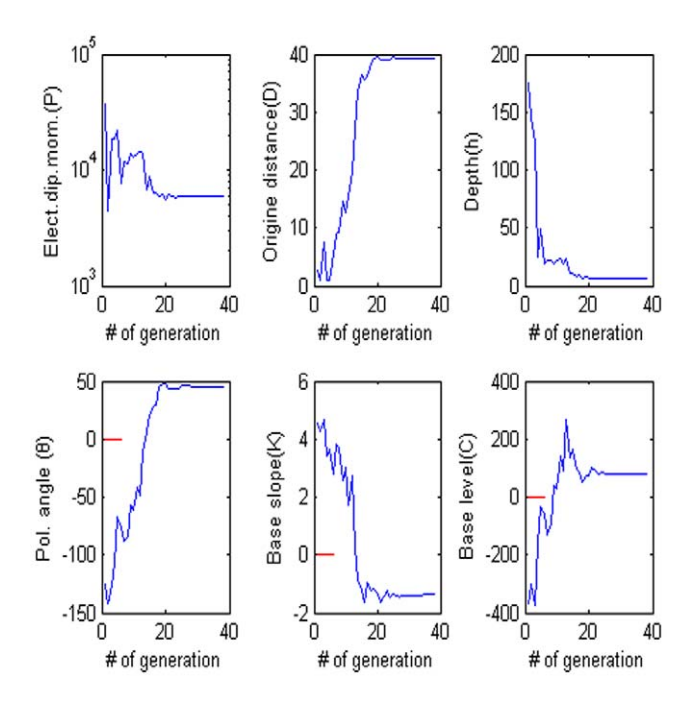


Figure 4. Values of each parameter versus the number of generation. (a) Amplitude P, (b) the distance from the origin D, (c) depth h, (d) polarization angle, (e) base slope K and (f) based level C. doi:10.1371/journal.pone.0051199.q004

Where $r_1, r_2, r_3, r_4, r_5 \in [1, \cdots, NP]$ are randomly chosen integers, and $r_1 \neq r_2 \neq r_3 \neq r_4 \neq r_5 \neq i$. F is the scaling factor controlling the amplification of the differential evolution. $X_{best,G}$ is the best individual vector with the best value in the population at generation G.

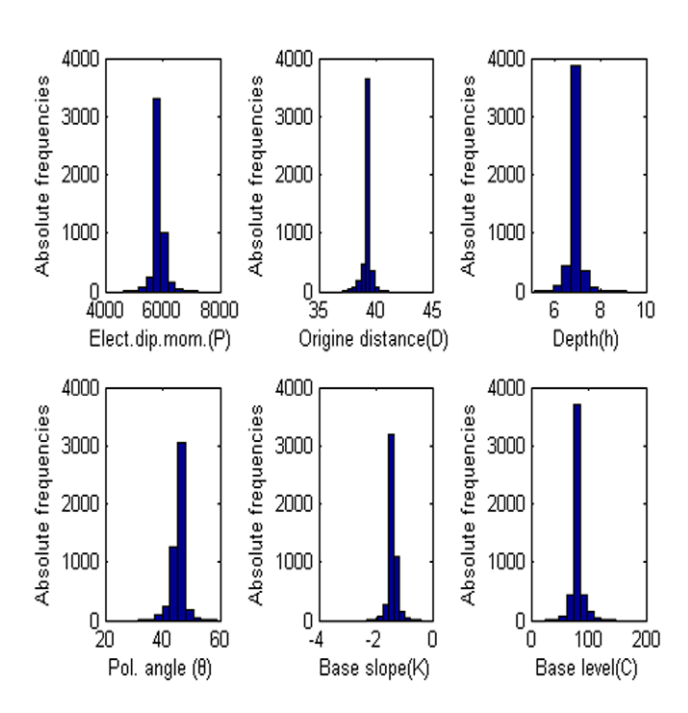


Figure 5. Frequency distribution of each parameter. (a) Amplitude P, (b) the distance from the origin D, (c) depth h, (d) polarization angle, (e) base slope K and (f) based level C. doi:10.1371/journal.pone.0051199.g005

Table 2. Comparison of true and estimated parameters of SP anomaly with 50% Gaussian noise caused by a cylinder model.

		DE			
Parameter True		Estimated	Statistics of DE		
Elect.dip.mom.	100,000	102700	Successes	30/30	
Distance	40	39.679	Mean iter.	36.43	
Depth	10	10.06	Std. iterations	7.19	
Pol. angle(degree)	60	59.186	Mean func. eval.	11230.00	
Base slope	0	-0.10591	Std func. eval.	2157.13	
Base level	0	9.5708	Std RMS	1.09	
			Mean RMS	13.54	
			Min RMS	13.2577	

doi:10.1371/journal.pone.0051199.t002

In the crossover operation, a recombination of the donor vector $V_{i,G}$ and the parent vector $X_{i,G}$ produce a trail vector $U_{i,G} = [u_{1,i,G}, u_{2,i,G}, u_{3,i,G}, \cdots, u_{D,i,G}]$. Basic DE employs the binomial crossover defined as follows:

$$u_{j,i,G} = \begin{cases} v_{j,i,G}, (rand_j[0,1] \le CR) or(j = j_{rand}) \\ x_{j,i,G}, otherwise \end{cases}$$
(4)

where $j = [1, \dots, D]$; $rand_j \in [0, 1]$ is a uniformly distribution distributed random number; $j_{rand} = [1, \dots, D]$ is the randomly chosen index, CR is the crossover rate $v_{j,i,G}$ is the difference vector of the jth particle in the ith dimension at the Gth iteration, and $u_{j,i,G}$ denotes the trail vector of the jth particle in the ith dimension at the Gth iteration.

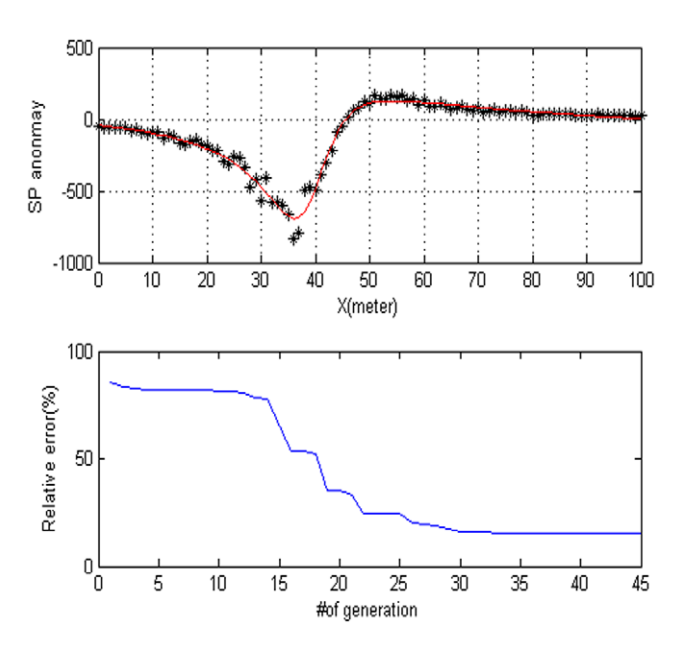


Figure 6. Contaminated synthetic data with 50% Gaussian noise for a cylinder. (a) Dotted lines synthetic data for a cylinder. Estimated SP anomaly is illustrated by solid line. (b) the convergence rate of the DE algorithm. doi:10.1371/journal.pone.0051199.g006

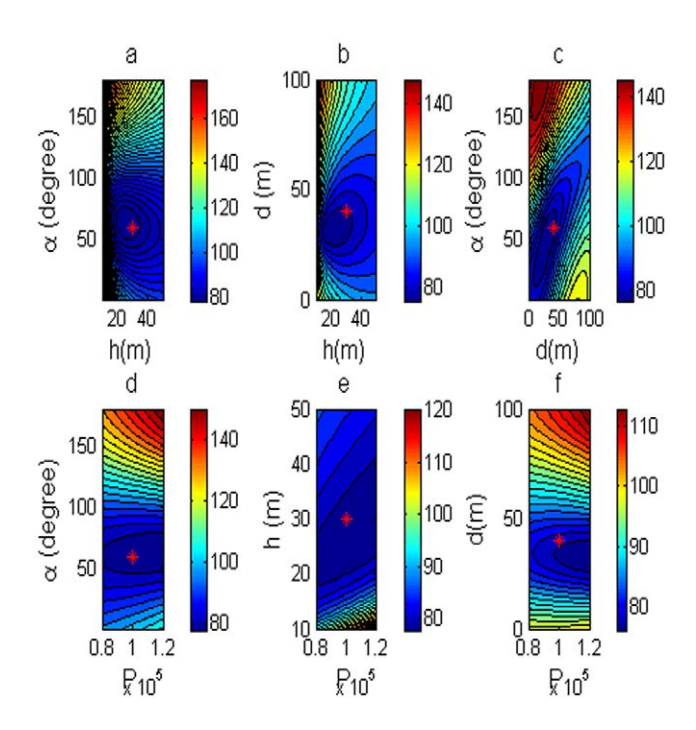


Figure 7. Contour maps of low misfit areas with noise free data. Two of six parameters are variable, rest of them are fixed. doi:10.1371/journal.pone.0051199.g007

Selection operator is used to choose the next population (i.e. G=G+1) between the trail population and the target population. The selection operation is described as:

$$X_{i,G+1} = U_{i,G}, \text{ If } f(U_{i,G}) \le f(X_{i,G})$$

= $X_{i,G}, \text{ If } f(U_{i,G}) > f(X_{i,G})$ (5)

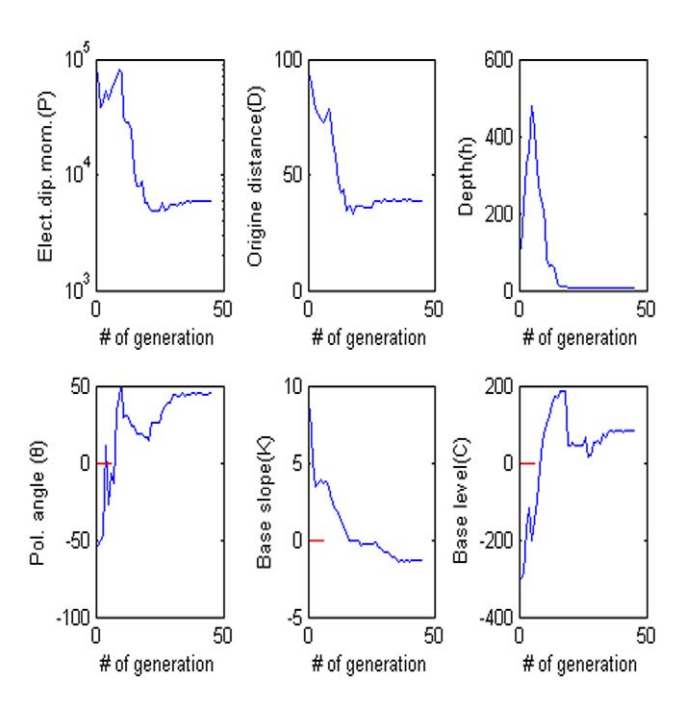


Figure 8. Values of each parameter versus the number of generation. (a) Amplitude P, (b) the distance from the origin D, (c) depth h, (d) polarization angle, (e) base slope K and (f) based level C. doi:10.1371/journal.pone.0051199.g008

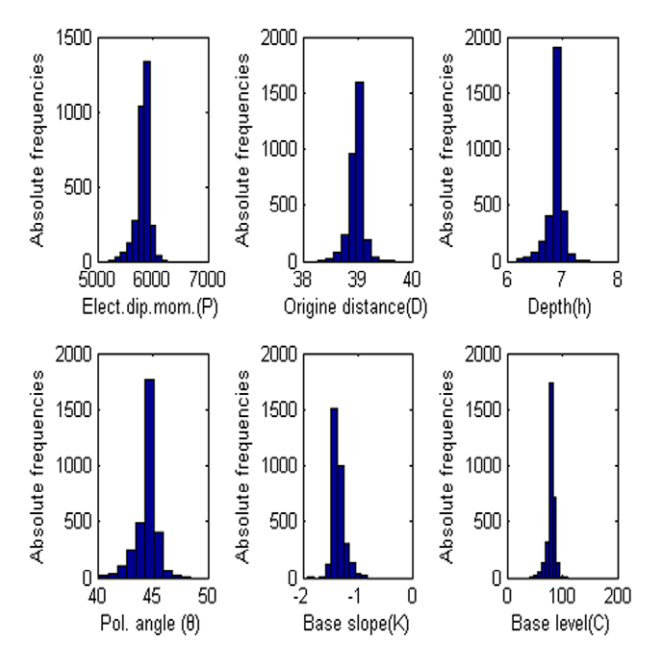


Figure 9. Frequency distribution of each parameter. (a) Amplitude P, (b) the distance from the origin D, (c) depth h, (d) polarization angle, (e) base slope K and (f) based level C. doi:10.1371/journal.pone.0051199.q009

The standard differential evolution algorithm can be described as the followings:

Procedure Algorithm description of DE algorithm

- 1: begin
- 2: Set the generation counter G = 0; and randomly initialize a population of NP individuals X_i . Initialize the parameter F, CR
- 3: Evaluate the fitness for each individual in *P*.

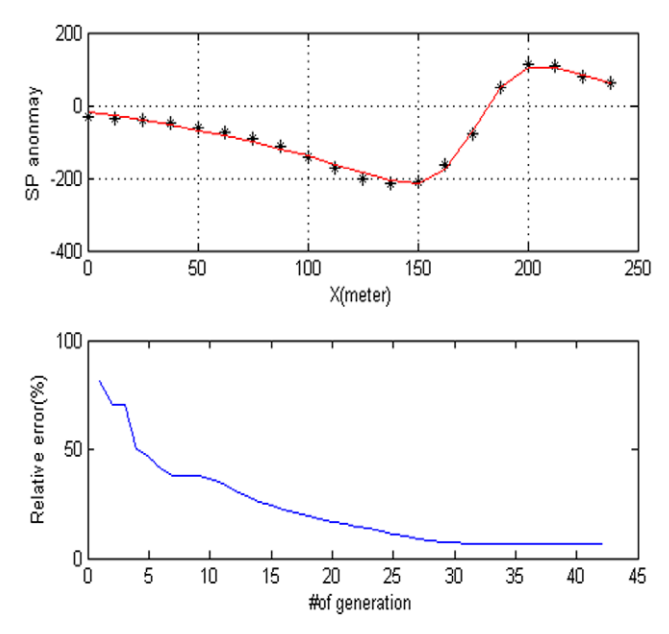


Figure 10. The data used here are digitized from Yungul (1950) algong A-M profile, it is called suleymankoy anomaly. doi:10.1371/journal.pone.0051199.g010

Table 3. PSO results and statistics of suleymankoy anomaly.

				Bhattacharya	Abdelrhman and			Ram Babu
Parameter	DE	PSO	Yungul	and Roy	Sharafeldin	El-Araby	Abdelrhman	and Rao
Elect.dip.mom.	11757	11704	-	-	-2458	-2661.2	-1549.3	-
Distance	76.73	77.21	76.70	70.00	-	-	_	66.36
Depth	32.661	32.501	38.00	40.00	42.00	47.63	38.78	41.40
Pol. angle(degree)	90.688	91.651	-69.00	-75.00	-77.00	-75.26	-75.33	-86.92
Base slope	-0.57907	-0.58242	0.00	0.00	-	-	-	0.22
Base level	47.016	45.559	0.00	0.00	-	-	_	43.00
PSO					DE			
Success	14/30	Std func. ev	al. 9984.21		Success	28/30	Std func. eval.	3647.83
Mean iter	62.71	Std RMS	12.19		Mean iter	43.00	Std RMS	9.58
Std. iterations	33.28	Mean RMS	16.85		Std. iterations	12.16	Mean RMS	14.65
Mean func. eval.	19114.29	Min RMS	6.5654		Mean func. eval.	13200.00	Min RMS	6.546

doi:10.1371/journal.pone.0051199.t003

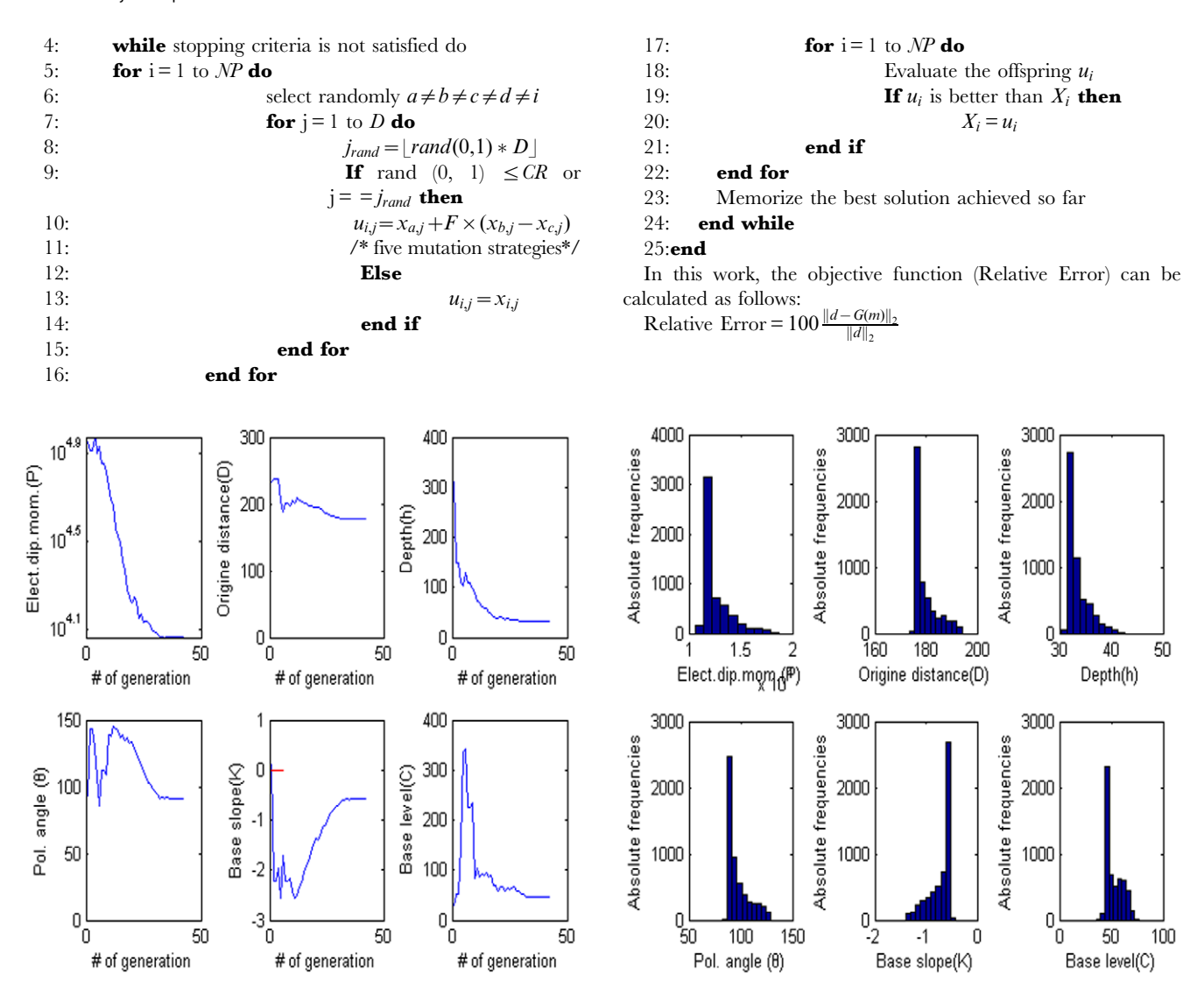


Figure 11. Values of each parameter versus the number of generation. (a) Amplitude P, (b) the distance from the origin D, (c) depth h, (d) polarization angle, (e) base slope K and (f) based level C. doi:10.1371/journal.pone.0051199.q011

Figure 12. Frequency distribution of each parameter. (a) Amplitude P, (b) the distance from the origin D, (c) depth h, (d) polarization angle, (e) base slope K and (f) based level C. doi:10.1371/journal.pone.0051199.g012

Table 4. DE results and statistics of Weiss anomaly.

Parameter	DE	PSO	Yungul	Bhattacharya and Roy	Abdelrhman an Sharafeldin	d El-Araby	Ram Babu and Rao
Elect.dip.mom.	-35406	-29461	-	-	-	-	-13253.80
Distance	96.155	101.57	105.70	108.20	-	-	109.83
Depth	47.883	44.453	53.80	54.00	52.90	43.37	61.05
Pol. angle(degree)	-62.102	-47.681	-64.00	-60.00	-54.70	-54.11	-56.17
Base slope	3.0699	1.9401	0.00	0.00	-	-	1.23
Base level	-219.14	-72.32	0.00	0.00	_	-	-5.48
PSO				DE			
Success	27/30	Std func. eval.	6397.01	Success	29/30	Std func. eval.	7679.60
Mean iter	48.07	Std RMS	1.63	Mean iter	40.43	Std RMS	8.15
Std. iterations	21.32	Mean RMS	11.58	Std. iterations	25.60	Mean RMS	14.99
Mean func. eval.	14722.22	Min RMS	9.8338	Mean func. eval.	12428.57	Min RMS	9.3594

doi:10.1371/journal.pone.0051199.t004

Results

In this paper, noise-free, contaminated and field data are used to demonstrate the performance and applicability of the proposed differential evolution and particle swarm optimization algorithm. The software is written in Matlab-7 language and experiments are made on a Pentium 3.0 GHz Processor with 1.0 GB of memory. In the parameter of PSO [25]: population size is 300. The number of generation is 100. e_1 and e_2 are set to be 1.8 and 2.0, respectively. And v_{max} is 5% of the search space. The inertia weight is set to 0.8. The following differential evolution parameters have been used after a number of careful experimentation: The population size is 300, the number of generation is 100, the scale factor F and crossover probability CR is 0.5, and 0.9, respectively. For the five mutation strategies of DE, "DE/current-to-best/1" was used in our experiment.

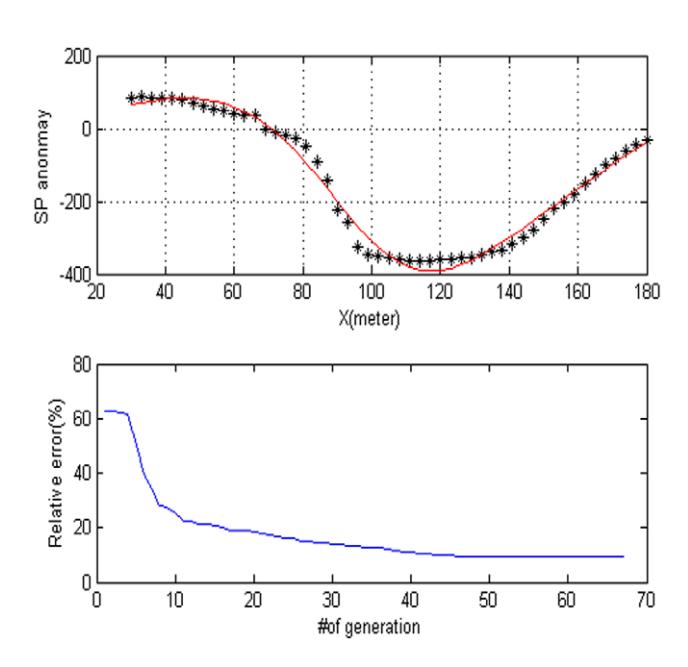


Figure 13. The data used here are digitized from Yungul (1950) algong A-M profile, it is called weiss anomaly. doi:10.1371/journal.pone.0051199.g013

Parameter ranges or the dimension of search space used here must be determined before the differential evolution process. The dimensions of the following ranges are used for the DE similar to the PSO: such as P being between -10,000 and 100,000, D being between 1 and maximum of x (the distance), h being between 0 and 500, θ set to -180 and 180° , M set to -20 and 20, and as for the last parameter C set to -1000 and 1000.

0.3 Noise-free Data

In this section, we will use the differential evolution for estimate a simple cylinder. The parameters of the model are polarization angle, the depth of the body center, the distance from the origin, the base slope, and the based level. First, we demonstrate some results with the synthetic data set for a cylinder model. The

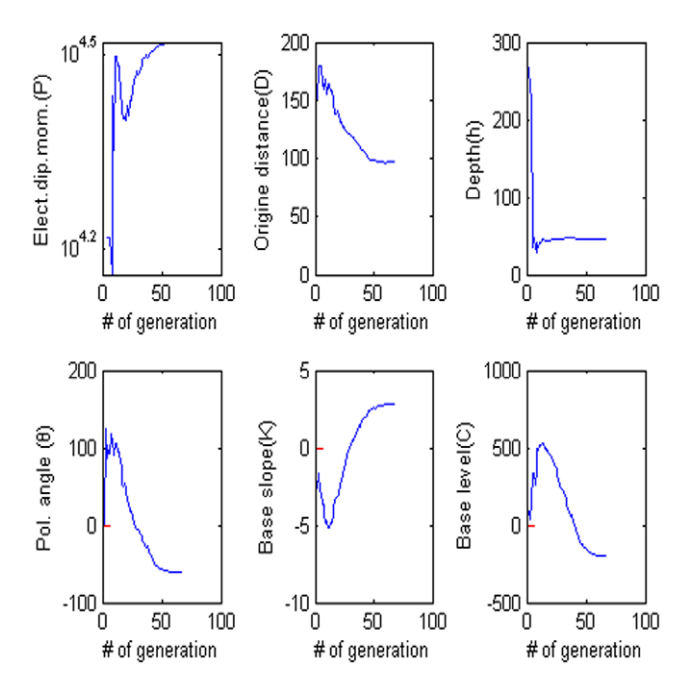


Figure 14. Values of each parameter versus the number of generation. (a) Amplitude P, (b) the distance from the origin D, (c) depth h, (d) polarization angle, (e) base slope K and (f) based level C. doi:10.1371/journal.pone.0051199.g014

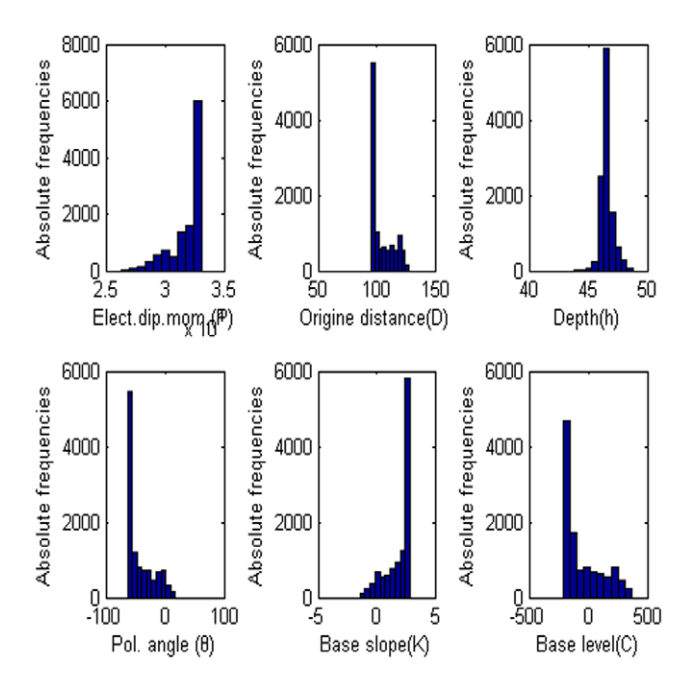


Figure 15. Frequency distribution of each parameter. (a) Amplitude P, (b) the distance from the origin D, (c) depth h, (d) polarization angle, (e) base slope K and (f) based level C. doi:10.1371/journal.pone.0051199.g015

experimental results of PSO and DE are shown in table 1. If the objective value if lower than the threshold value with 0.1% on the two iterations, then we think it is success. In table 1, the true values represent the correct values of parameters with the purpose of comparison. The estimated values are given in third column. The successes rate, mean iteration, std. iterations, mean function evaluation, std. function evaluation, std. RMS, mean RMS and Min RMS of PSO and DE are listed in column four and column seven. Compared with the PSO algorithm, we find that the DE algorithm can provide smaller RMS (0.001578) than PSO algorithm with little iterations. For the success rate, DE algorithm can obtain all conditions. The anomaly of the corresponding model is shown in Figure 2. Figure 2(a) shows the model response. Figure 2(b) shows the fitness behavior. From figure 2(b), after 50 generations, there are no significant changes.

The inverse problem has 6 unknown parameters need to be solved. The problem is a simple 2-dimension problem. In order to

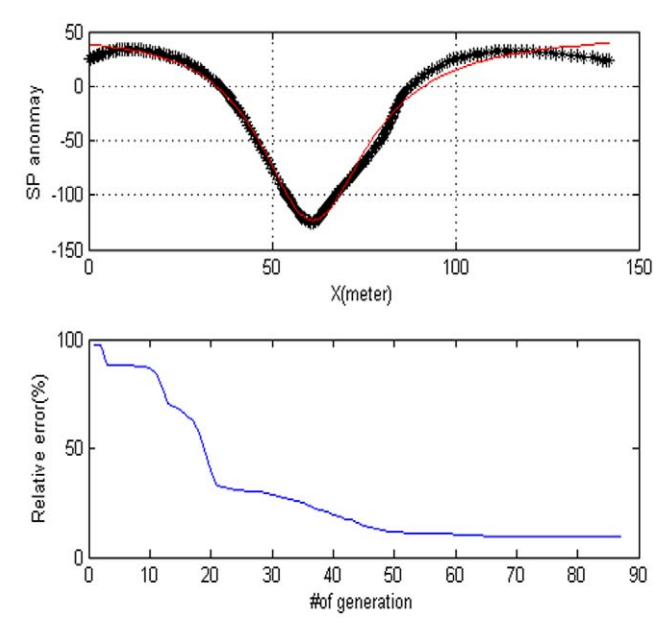


Figure 16. The data used here are digitized from Yungul (1950) algong A-A' profile, it is called Nalbant cesmesi anomaly. doi:10.1371/journal.pone.0051199.q016

dissent the performance of errors for estimating the model parameter by using the DE, Figure 3 shows the polarization angle and the depth of the body center as variables. Then, two of six parameters are variables, and the rest are fixed as P=100,000, D=40 m, h=30 m, $\theta=60^{\circ}$, M=0, and C=0. The low misfit area and the exact point on the map use a star to express it. The rest of the panels are also shown in Figure 3. Figure 4(a–f) shows the behavior of the corresponding parameters. Figure 5 shows high frequencies with the respect to the correct value of parameters.

0.4 Contaminated Synthetic Data

Noisy data plays an important role in both geophysics and other sciences as well. In order to analyze the behavior of noise corrupted data, we will add some noise to the data set. Figure 6 shows the anomaly of the corresponding model. The parameter obtained from the DE inversions considering noise free data with Gaussian noise added on the values are shown in Table 2. Figure 7 shows the contour maps that illustrate the low misfit area and the

Table 5. DE results and statistics of Nalbant cesmesi anomaly.

				PSO		DE	
Parameter	DE	PSO	Abdelrhman et al	Estimated	Statistics of PSO	Estimated	Statistics of DE
Elect.dip.mom.	84806	84597	3403.12	Successes	14/30	Successes	22/30
Distance	59.754	60.121	-	Mean iter.	66.64	Mean iter.	45.86
Depth	22.702	22.699	26.23	Std. iterations	21.24	Std. iterations	16.87
Pol. angle(degree)	-10.401	-8.5744	-68.53	Mean func. eval.	20292.86	Mean func. eval.	14059.09
Base slope	0.017072	0.014053	-	Std func. eval.	6371.14	Std func. eval.	5061.87
Base level	40.042	40.492	-	Std RMS	4.50	Std RMS	6.36
				Mean RMS	10.19	Mean RMS	9.85
				Min RMS	8.1106182767	Min RMS	8.0862

doi:10.1371/journal.pone.0051199.t005

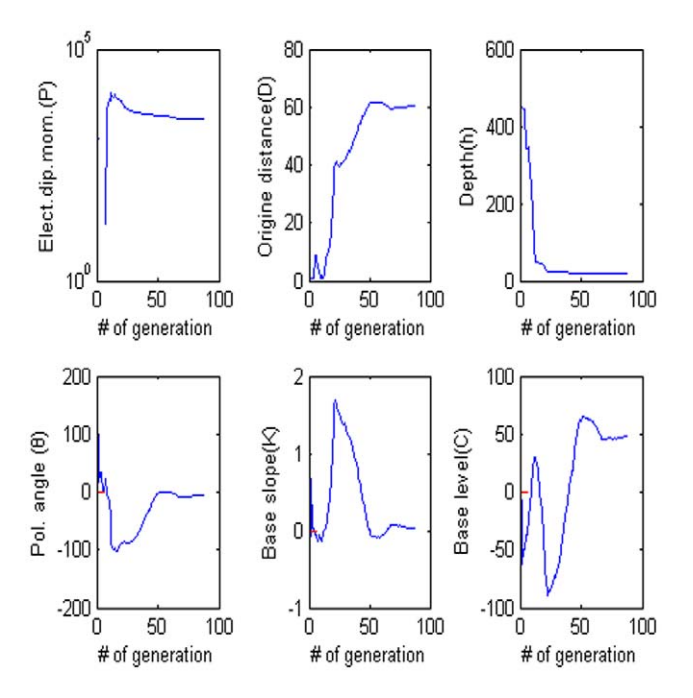


Figure 17. Values of each parameter versus the number of generation. (a) Amplitude P, (b) the distance from the origin D, (c) depth h, (d) polarization angle, (e) base slope K and (f) based level C. doi:10.1371/journal.pone.0051199.q017

exact point the map with a star. Figure 8 shows the behavior of the corresponding parameters. According to the frequency distribution, the mode of the histogram provided the correct parameter values. Figure 9 show the high frequency with the respect to the correct value of parameters. It can be noted that the parameters are quite well recovered from the DE inversion.

0.5 Süleymanköy Anomaly

Süleymanköy anomaly is a quite well-known data set in the literature. The length of profile is 237.5 m. Data are digitized at intervals of 12.5 m along the profile. The algorithm has been executed for 30 times with differential initial populations and the

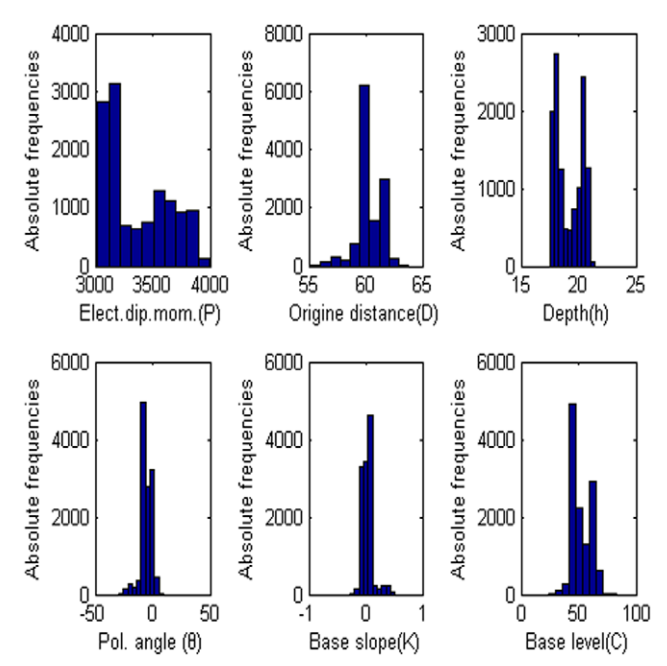


Figure 18. Frequency distribution of each parameter. (a) Amplitude P, (b) the distance from the origin D, (c) depth h, (d) polarization angle, (e) base slope K and (f) based level C. doi:10.1371/journal.pone.0051199.g018

experimental result as the final optimization solution has been selected. The experimental results obtained from the DE are compared with those obtained by using other algorithms including Yungul (1950), Bhattacharya and Roy (1981), Rarm Babu and Rao (1981), Abdelrahman and sharafeldin (1997), Abedlrahman et al.(1997a), El-Araby (2004), Peksen et al (2010) [13,24–29] in terms of different parameter, in Table 3, which shows that DE successes in finding the best solutions for the test methods. Compared with the PSO algorithm, the DE algorithm can provide better solutions than PSO algorithm. The DE can provide 28 successes rate compared with the 14 times of PSO. For the DE algorithm, the parameters are set as follows: the polarization angle

Table 6. Compared with other state of the art DE algorithms.

problems	Algorithms	Successes	Mean iter.	Std. iterations	Mean func. eval.	Std func. eval.	Std RMS	Mean RMS	Min RMS
suleymankoy anomaly	DE	28/30	43.00	12.16	13200.00	3647.83	9.58	14.65	6.546
	jDE	10/30	29.20	8.00	9060.00	2399.17	4.47	33.51	26.465
	DE/BBO	8/30	63.63	36.04	19387.50	10811.8	4.10	35.53	27.692
	JADE	2/30	12.50	2.12	4050.00	636.40	1.06	39.06	38.305
Weiss anomaly	DE	29/30	40.43	25.60	12428.57	7679.60	8.15	14.99	9.3594
	jDE	5/30	11.20	4.44	3660.00	1331.54	2.48	36.35	34.167
	DE/BBO	10/30	76.40	39.80	23220	11940.0	5.65	31.91	22.635
	JADE	3/30	10.67	4.73	3500.00	1417.74	5.10	31.19	26.747
Nalbant cesmesi anomaly	DE	22/30	45.86	16.87	14059.09	5061.87	6.36	9.85	8.0862
	jDE	15/30	35.80	13.84	11040.00	4152.59	7.60	23.37	8.405
	DE/BBO	7/30	101.0	29.56	30600	8869.05	13.16	23.16	8.323
	JADE	1/30	28.00	0.00	8700.00	0.00	0.00	37.00	37.001

doi:10.1371/journal.pone.0051199.t006

 θ = -90.688, the electrical dipole moment is P=11,757 mV, the depth of the body center is 32.661, the distance is 176.73 m and the best fitness 6.55. The DE algorithm and the Süleymanköy anomaly are given in Figure 10(a). The convergence rate for the proposed algorithm for the corresponding anomaly is depicted in Figure 10(b). In this model, we use the sphere model. Figure 11 shows the behavior of each parameter. Figure 12 shows the frequency distribution of each parameter by using Süleymanköy anomaly.

0.6 Weiss Anomaly

Weiss anomaly is a quiet well-known data set in the literature. The algorithm has been executed for 30 times with differential initial populations and the experimental result as the final optimization solution has been selected. The experimental results obtained from the DE are compared with those obtained by using other algorithms including Yungul (1950), Bhattacharya and Roy (1981), Rarm Babu and Rao (1988), Abdelrahman and sharafeldin (1997), El-Araby (2004), Peksen et al (2010) [13,25-28] in terms of different parameter, in Table 4, which shows that DE can beat other algorithms. Compared with the PSO algorithm, the DE algorithm can provide better solution than PSO algorithm. The DE can provide 29 successes rate than the 27 times of PSO. For the DE algorithm, the parameters set as follows: the polarization angle $\theta = -62.102$, the electrical dipole moment is P = -35,406 mV, the depth of the body center is 47.883, the distance is 96.155 m and the best fitness 9.36 better than the best fitness 9.83 of PSO algorithm. Figure 13a and b show digitized the DE algorithm and the Weiss anomaly and the convergence rate for the proposed algorithm for the corresponding anomaly, respectively. In this model, we also use the sphere model. Figure 14 shows the behavior of each parameter. Figure 15 shows the frequency distribution of each parameter by using Weiss anomaly.

0.7 Nalbant Cesmesi Anomaly

In this section, we will use the DE algorithm to estimate the parameter of Nalbant cesmesi anomaly. The algorithm has been executed for 30 times with differential initial populations and the experimental results as the final optimization solution have been selected. The experimental results obtained from the DE are compared with those obtained by using other algorithms including Yungul (1954), Abedelrahman et al (2008), Peksen et al (2010) [25,30-31] in terms of different parameters, in Table 5, which shows that DE can beat other algorithms. In this model, we also use the horizontal cylinder model. Compared with the PSO algorithm, the DE algorithm can provide better solution than PSO algorithm. The DE can provide 22 successes rate than the 14 times of PSO. For the DE algorithm, the parameters are set as follows: the polarization angle $\theta = -8.5744$, the electrical dipole moment is P = 84597 mV, the depth of the body center is 22.699, the distance is 60.121 m and the best fitness is 8.08 better than the best fitness 8.10 of PSO algorithm. Figure 16(a) shows that anomaly along the profile and Figure 16(b) shows the fitness value versus the number of generation. Figure 17 shows the behavior of

References

- Goldie M (2002) Self-potentials associated with the Yanacocha high-sulfidation gold deposit in Peru Geophysics, 67, 684

 –689.
- Mendonça CA (2008) Forward and inverse modeling in mineral exploration. Geophysics 73, F33-F43.
- Wynn JC, Sherwood SI (1984) The Self-Potential (SP) method: an inexpensive reconnaissance and archaeological mapping tool Journal of Field Archaeology, 11, 195–204.

each parameter. Figure 18 shows the frequency distribution of each parameter by using Nalbant cesmesi anomaly.

Discussion

0.8 Compared with Other State of the Art DE Algorithms

In order to evaluate the effectiveness and efficiency of our method, we further compare its performance with some state-ofart DE algorithms. They are jDE [16], DE/BBO [19] and JADE [32]. jDE is a improved version of DE by proposing a self adaptive parameter setting in differential evolution to avoid the manual parameter setting of F and CR. The parameter control technique is based on the self adaptation of two parameters associated with the evolutionary process. DE/BBO is a hybrid differential evolution algorithm, which hybridizes the DE operator with the migration of BBO. In JADE, a normal distribution and a Cauchy distribution are utilized to generate F and CR for each target vector, respectively. Table 6 summarizes the experimental results. As can be seen in this table, surprisingly, the standard DE significantly outperforms the up-to-date DE algorithms for suleymankoy anomaly, Weiss anomaly and Nalbant cesmesi anomaly. For the suleymankoy anomaly, DE can provide 28 successes rate compared with the 10, 8, 2 times of jDE, DE/BBO and JADE. For Weiss anomaly, DE can win 29 successes rate compared with the 5, 10, 3 times of jDE, DE/BBO and JADE. For Nalbant cesmesi anomaly, DE can generate better solutions than other algorithms and provide 22 successes rate.

Though standard DE performs much better than these up-to-date DE variants do, it does not mean that standard DE is better than these algorithms. The reason may be that jDE, DE/BBO and JADE are all designed for the purpose of solving general unconstrained problems. Yet, in this paper, the self potential data problem is very specific. This also brings us an open problem: can the researchers propose some improved version of DE on solving the self potential data problem?

Conclusions

This paper illustrated the application of differential evolution in estimating the self-potential data. The effectiveness of the proposed algorithm is demonstrated on three difficult instances including noise free data, contaminated synthetic data and some field data. The DE algorithm has the ability to find the better quality solution, and has better convergence characteristics and computational efficiency. The comparison of the results with other methods reported in the literature show the superiority of the proposed method and its potential for solving SP problem. From the results obtained, it is concluded DE algorithm is a promising technique for solving the quantitative interpretation of self potential data. In the future work, we will try to propose some improved version of DE to solve the problem.

Author Contributions

Conceived and designed the experiments: MY. Performed the experiments: XL. Analyzed the data: XL. Contributed reagents/materials/analysis tools: XL. Wrote the paper: XL.

- Hunter L, Powers M (2008) Geophysical Investigations of Earthen Dams: An Overview, 21th SAGEEP, 1083–1096.
- Quarto R, Schiavone D (1996) Detection of cavities by the self-potential method First Break. 14, 419–430.
- Vichabian Y, Morgan FD (2002) Self potentials in cave detection The leading edge, 21, 866–871.
- Corwin RF, Hoover DB (1979) The self-potential method in geothermal exploration. Geophysics 44, 226–245.

- Minsley BJ, Coles DA, Vichabian Y, Morgan FD (2008) Minimization of self potential survey mis-ties acquired with multiple reference locations. Geophysics 73, F71–F81.
- Paul MK (1965) Direct interpretation of self-potential anomalies caused by inclined sheets of infinite extension Geophysics, 30, 418

 –423.
- Meiser P (1962) A method of quantitative interpretation of self-potential measure-ments. Geophysical Prospection 10, 203–218.
- Murthy BVS, Haricharan P (1985) Nomograms for the complete interpretation of spontaneous potential profiles over sheet like and cylindrical 2D structures. Geophysics 50,1127–1135.
- Abdelrahman EM, El-Araby TM, Essa KS (2009) Shape and depth determinations from second moving average residual self-potential anomalies. Journal of Geophysics and Engineering 6, 43–52.
- El-Araby H (2004) A new method for quantitative interpretation of self-potential anomalies. Journal of Applied Geophysics 55, 211–224.
- Abdelrahman EM, El Araby HM, El Araby TM, Hassaneen AG, Hafez MA (2003) New methods for shape and depth determinations from SP data Geophysics 68 1202–10.
- Storn R, Price K (1997) Differential evolution-a simple and efficient heuristic for global optimization over continuous space, Journal of Global Optimization.11 (1), 341–359.
- Brest J, Greiner S, Boskovic B, Mernik M, Zumer V (2006) Self adapting control parameters in differential evolution: A comparative study on numerical benchmark problems, IEEE Transactions on Evolutionary Computation, 10(6), 647–657.
- Rahnamayan S, Tizhoosh HR, Salama MMA (2008) Opposition-based differential evolution, IEEE Transactions on Evolutionary Computation, 12(1),64–79.
- Qin AK, Huang VL, Suganthan PN (2009) Differential evolution algorithm with strategy adaptation for global numerical optimization, IEEE Transactions on Evolutionary Computation, 13, 398–417.
- Gong W, Cai Z, Ling C (2010) DE/BBO: A hybrid differential evolution with biogeography-based optimization for global numerical optimization, Soft Computing, 15, 645–665.

- Li X, Yin M (2011) Hybrid Differential Evolution with Biogeography based Optimization for Design of a Reconfigurable Antenna Array with Discrete Phase Shifters. International Journal of Antennas and Propagation, Article ID 685629.
- Gong WY, Cai ZH, Jiang LX (2008) Enhancing the performance of differential evolution using orthogonal design method, Applied Mathematics and Computation, 206, 56–69.
- Wang JN, Xu HL, Sun SL, Gao T, Li HZ, et al. (2012) An effective method for accurate prediction of the first hyperpolarizability of alkalides. Journal of Computational Chemistry 33(2), 231–236.
- Neri F, Tirronen V (2009) Scale Factor Local Search in Differential Evolution, Memetic Computing Journal, 1(2), 153–171.
- 24. Rao BSR, Murthy IVR, Reddy SJ (1970) Interpretation of self-potential anomalies of some simple geometrical bodies Pure and Applied Geophysics, 78, 60–77
- Peksen E, Yas T, Yekta kayman A, Ozkan C (2011) Application of particle swarm optimization on self potential data, journal of applied Geophysics, 75.305–318.
- Yüngül S (1950) Interpretation of spontaneous-polarization anomalies caused by spherical ore bodies Geophysics, 15, 237–246.
- Bhattacharya BB, Roy N (1981) A note on the use of a nomogram for selfpotential anomalies Geophys. Prospect. 29 102–7.
- Abdelrahman EM, El-Araby TM, Ammar AA, Hassanein HI (1997a) A least-squares approach to shape determination from self-potential anomalies Pure Appl. Geophys. 150 121–8.
- Abdelrahman EM, Ammar AA, Sharafeldin SM, Hassanein HI (1997a) Shape and depth solutions from numerical horizontal self-potential gradients Appl. Geophys. 36 31–43.
- 30. Yüngül S (1954) Spontaneous potential survey of a copper deposit at Sanyer, Turkey Geophysics, 19, 455–458.
- Abdelrahman EM, Essa KS, Abo-Ezz ER, Sultan M, Sauck WA, et al. (2008) New least-squares algorithm for model parameters estimation using self-potential anomalies. Computers and Geosciences 34, 1569–1576.
- Zhang JQ, Sanderson AC (2009) JADE: Adaptive Differential Evolution With Optional External Archive, IEEE Trans on Evolutionary Computation, 13(5), 945–958